Korean J. Chem. Eng., **23**(1), 8-16 (2006)

Systematics and modelling representations of LPG thermal cracking for olefin production

Jafar Towfighi, Aligholi Niaei*,†, Ramin Karimzadeh and Giti Saedi

ORG, Dept. of Chem. Eng., Tarbiat Modares University, P.O.Box 14115-143, Tehran, Iran
*Petroleum Res. Lab., Dept. of Chem. Eng., University of Tabriz, 51666 16471, Tabriz, Iran
(*Received 15 June 2005 • accepted 7 September 2005*)

Abstract–Pyrolysis of hydrocarbons is an important commercial process for the production of ethylene, propylene and 1,3 butadiene. These low molecular weight olefins are among the most important base chemicals for the petrochemical industries for polymer production. A simulation program of the reaction kinetics and coke formation inside the coils of a thermal cracking unit can provide information on the effects of operating conditions on the product distribution. The aim of this study was to develop a mechanistic reaction model for the pyrolysis of LPG that can be used to predict the yields of the major products from a given LPG sample with commercial indices. A complete reaction network, using a rigorous kinetic model, for the decomposition of the LPG feed has been developed, which is used for the simulation of industrial LPG crackers. This model has been adapted using industrial data for the pyrolysis yields of LPG. The present paper attends on the asymptotic coking mechanism and describes the development of a kinetic coking model in the pyrolysis of LPG. Detailed and accurate information about the product distribution, growth of coke layer, the evolution of the tube skin temperatures can be obtained from this simulation. Simulations of this kind can be used to optimize the furnace operation. They can be used as a guide for the adaptation of the operating variables aiming at prolonging the run length of the furnace. The reactor model, as well as kinetic scheme, is tested in an industrial cracking furnace.

Key words: LPG, Modelling, Cracking Furnace, Coke Deposition, Olefin

INTRODUCTION

Thermal cracking of light hydrocarbons such as ethane, propane, n-Butane, i-Butane and their mixture of the main processes for the production of olefins. The feed, ranging from light gaseous hydrocarbons to gas oil, is cracked in 4-8 tubular coils suspended in a fired rectangular furnace. The heat required for the endothermic reactions is provided via radiation burners in the sidewall or long flame burners in the bottom of the furnace. Mathematical models describing the simulation of the pyrolysis reactors need to be combined with complex kinetic models with important features such as coking, heat and mass transfer, firebox profiles and fluid dynamic characteristics. The central part of the model is the kinetic mechanism and related constants. Typically, the chemistry component can consist of several hundred reactions involving large numbers of species, and this together with the coupling of the kinetic rate equations to the physical features can lead to computationally difficult calculations. The use of full kinetic mechanisms for on-line simulations such as plant optimisation is therefore rarely possible in order to obtain a favourable product distribution or to reduce unwanted side effects. The present paper describes the development of a kinetic reaction network for the pyrolysis of LPG, and with the help of an accurate coking kinetic model, the calculation of the temperature and product distribution in the reactor length and run time can be achieved. Simultaneous simulation of the reactor and the firebox provides a detailed understanding of the behaviour of the cracking furnace. The experimental pilot results and simulation for the LPG cracking are in good agreement with the industrial data.

†To whom correspondence should be addressed.
E-mail: niaei@yahoo.com, a.niaei@tabrizu.ac.ir

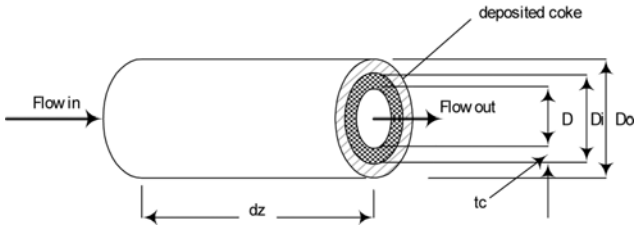

Fig. 1. Differential element of a cracking coil.

MODEL EQUATIONS

1. Reactor Model

A one dimensional plug flow model is used to simulate the thermal cracking reactor. The steady state spatial equations for the coils are given below [Dente et al., 1979; Heynderickx and Froment, 1998]. The geometry of the reactor model configuration is shown in Fig. 1.

Assumptions:
(1) One dimensional flow
(2) Plug flow
(3) Radial concentration gradients and axial dispersion are negligible
(4) Ideal gas behaviour
(5) Inertness of the steam diluent in feed
(6) No hydrodynamic or thermal entrance region effects
(7) Quasi steady state in Coke deposition model.

In this form, the coking rate model is pseudo steady state with respect to time. In other words, coking rate is assumed constant over a time step and the effect of coke formation through coking equation is updated explicitly at the end of each time step. This pseudo

Table A1. Typical reactions of pyrolysis of ethane, propane, n-butane, i-butane and their mixtures

Reaction	Log A	E (Kcal/mol)	Reaction	Log A	E (Kcal/mol)
$C_2H_6 \rightarrow CH_3+CH_3$	16.1	87.5	$C_3H_8+H \rightarrow C_3H_7+H_2$	11.0	9.70
$nC_4H_{10} \rightarrow C_2H_5+C_2H_5$	16.2	82.10	$C_3H_8+H \rightarrow 2C_3H_7+H_2$	11.0	8.30
$nC_4H_{10} \rightarrow C_3H_7+CH_3$	17.0	85.40	$C_3H_6+CH_3 \rightarrow aC_3H_5+CH_4$	9.3	12.20
$C_4H_8 \rightarrow aC_3H_5+CH_3$	15.5	74.00	$C_3H_8+CH_3 \rightarrow C_3H_7+CH_4$	10.5	11.50
$C_2H_4+H \rightarrow C_2H_3+H_2$	8.9	4.00	$C_3H_8+CH_3 \rightarrow 2C_3H_7+CH_4$	9.6	10.10
$C_2H_6+H \rightarrow C_2H_5+H_2$	11.0	9.70	$C_3H_6+C_2H_3 \rightarrow aC_3H_5+C_2H_4$	9.5	14.50
$C_2H_4+CH_3 \rightarrow C_2H_3+CH_4$	10.0	13.00	$C_3H_8+C_2H_3 \rightarrow C_3H_7+C_2H_4$	9.5	18.80
$C_2H_6+CH_3 \rightarrow C_2H_5+CH_4$	11.6	16.50	$C_3H_8+C_2H_3 \rightarrow 2C_3H_7+C_2H_4$	9.0	16.20
$C_2H_4+C_2H_5 \rightarrow CH_3+C_3H_6$	9.7	19.00	$C_3H_6+C_2H_5 \rightarrow aC_3H_5+C_2H_6$	8.0	9.20
$C_2H_3 \rightarrow C_2H_2+H$	9.7	31.50	$C_3H_8+C_2H_5 \rightarrow C_3H_7+C_2H_6$	9.1	12.60
$C_2H_5 \rightarrow C_2H_4+H$	13.3	40.00	$C_3H_8+C_2H_5 \rightarrow 2C_3H_7+C_2H_6$	8.9	10.40
$aC_3H_5 \rightarrow C_2H_2+CH_3$	10.5	36.20	$C_3H_8+aC_3H_5 \rightarrow C_3H_7+C_3H_6$	9.0	18.80
$C_3H_7 \rightarrow C_2H_4+CH_3$	13.6	32.60	$C_3H_8+aC_3H_5 \rightarrow 2C_3H_7+C_3H_6$	8.9	16.20
$C_3H_7 \rightarrow C_3H_6+H$	13.3	38.40	$2C_3H_7 \rightarrow C_3H_6+H$	13.3	38.70
$aC_4H_7 \rightarrow C_4H_6+H$	13.5	49.30	$C_4H_9 \rightarrow C_3H_6+CH_3$	13.4	31.90
$aC_4H_7 \rightarrow C_2H_4+C_2H_3$	11.0	37.00	$C_3H_6+CH_3 \rightarrow C_4H_9$	8.5	9.10
$C_4H_9 \rightarrow C_2H_4+C_2H_5$	12.4	28.00	$C_2H_4+2C_3H_7 \rightarrow C_5H_{11}$	7.1	6.90
$C_4H_9 \rightarrow C_4H_8+H$	13.0	36.60	$2C_3H_7+H \rightarrow C_3H_8$	13.3	0.00
$C_5H_{11} \rightarrow C_{10+}+H$	11.6	36.60	$C_3H_7+CH_3 \rightarrow nC_4H_{10}$	9.5	0.00
$C_5H_{11} \rightarrow C_4H_8+CH_3$	14.5	31.50	$2C_3H_7+CH_3 \rightarrow nC_4H_{10}$	9.5	0.00
$C_5H_{11} \rightarrow C_2H_4+1C_3H_7$	10.6	40.00	$aC_3H_5+aC_3H_5 \rightarrow C_{10+}$	9.5	0.00
$C_2H_2+H \rightarrow C_2H_3$	10.6	1.30	$CO+H_2O \rightarrow CO_2+H_2$	14.5	62.00
$C_2H_4+H \rightarrow C_2H_5$	10.0	1.50	$CO_2+H_2 \rightarrow CO+H_2O$	14.5	70.00
$C_3H_6+H \rightarrow C_3H_7$	10.0	2.90	$C_2H_2+H_2O \rightarrow CO+H_2$	14.4	62.00
$C_4H_6+H \rightarrow aC_4H_7$	10.8	1.30	$CH_4+H_2O \rightarrow CO+H_2$	10.4	64.00
$C_2H_4+CH_3 \rightarrow C_3H_7$	8.3	7.90	$C_2H_4+H_2O \rightarrow CO+H_2$	10.8	68.00
$C_2H_4+C_2H_3 \rightarrow aC_4H_7$	7.7	7.00	$C_4H_8+H \rightarrow aC_4H_7+H_2$	10.7	3.90
$C_2H_4+C_2H_5 \rightarrow C_4H_9$	7.2	7.60	$C_4H_8+CH_3 \rightarrow aC_4H_7+CH_4$	8.0	7.30
$C_3H_6+C_2H_5 \rightarrow C_5H_{11}$	7.1	7.50	$2C_4H_9 \rightarrow C_3H_6+CH_3$	13.4	31.90
$C_2H_4+C_3H_7 \rightarrow C_5H_{11}$	7.3	7.40	$2C_4H_9 \rightarrow C_4H_8+H$	13.3	39.80
$C_2H_3+H \rightarrow C_2H_4$	10.0	0.00	$C_5H_{11} \rightarrow C_5H_{10}+H$	13.7	36.60
$C_2H_5+H \rightarrow C_2H_6$	10.6	0.00	$C_3H_6+H \rightarrow 2C_3H_7$	10.0	1.50
$aC_3H_5+H \rightarrow C_3H_6$	10.3	0.00	$C_4H_8+H \rightarrow 2C_4H_9$	10.0	1.20
$C_3H_7+H \rightarrow C_3H_8$	11.7	0.00	$C_3H_6+CH_3 \rightarrow iC_4H_9$	8.5	9.10
$aC_4H_7+H \rightarrow C_4H_8$	10.6	0.00	$2C_4H_9+H \rightarrow nC_4H_{10}$	10.0	0.00
$C_4H_9+H \rightarrow nC_4H_{10}$	10.7	0.00	$C_5H_{11}+H \rightarrow nC_5H_{12}$	10.0	0.00
$C_5H_{11}+H \rightarrow C_{10+}$	7.0	0.00	$4C_4H_7+CH_3 \rightarrow C_6H_{12}$	9.5	0.00
$CH_3+CH_3 \rightarrow C_2H_6$	10.1	0.00	$4C_4H_7+C_2H_3 \rightarrow C_6H_{12}$	9.1	0.00
$C_2H_5+CH_3 \rightarrow C_3H_8$	11.0	0.00	$aC_3H_5+C_2H_5 \rightarrow C_6H_{12}$	9.5	0.00
$aC_3H_5+CH_3 \rightarrow C_4H_8$	10.5	0.00	$C_3H_7+C_2H_5 \rightarrow C_6H_{12}$	8.9	0.00
$aC_4H_7+CH_3 \rightarrow C_{10+}$	7.8	0.00	$2C_3H_7+C_2H_5 \rightarrow C_6H_{12}$	8.9	0.00
$C_2H_3+C_2H_3 \rightarrow C_4H_6$	9.6	0.00	$4C_4H_7+C_2H_5 \rightarrow C_6H_{12}$	9.5	0.00
$aC_4H_7+C_2H_3 \rightarrow C_{10+}$	8.3	0.00	$aC_3H_5+aC_3H_5 \rightarrow C_6H_{12}$	9.5	0.00
$C_2H_5+C_2H_5 \rightarrow nC_4H_{10}$	9.6	0.00	$4C_4H_7+aC_3H_5 \rightarrow C_6H_{12}$	10.1	0.00
$C_2H_5+C_2H_5 \rightarrow C_2H_4+C_2H_6$	7.7	0.00	$4C_4H_7+4C_4H_7 \rightarrow C_6H_{12}$	9.1	0.00
$aC_4H_7+C_2H_5 \rightarrow C_{10+}$	7.7	0.00	$iC_4H_{10} \rightarrow 2C_3H_7+CH_3$	16.3	82.00
$aC_4H_7+aC_3H_5 \rightarrow C_{10+}$	8.3	0.00	$2C_4H_8 \rightarrow aC_3H_5+CH_3$	16.3	71.30
$aC_4H_7+aC_4H_7 \rightarrow C_{10+}$	7.7	0.00	$2C_4H_8+H \rightarrow aC_4H_7+H_2$	10.7	3.80
$C_4H_6+C_2H_2 \rightarrow BENZ+H_2$	9.6	22.50	$iC_4H_8+H \rightarrow iC_4H_7+H_2$	10.5	3.80
$C_4H_6+C_3H_4 \rightarrow H_2+TOLUENE$	8.9	22.50	$iC_4H_{10}+H \rightarrow iC_4H_9+H_2$	11.0	8.40
$C_3H_4+H \rightarrow aC_3H_5$	10.7	2.00	$2C_4H_8+CH_3 \rightarrow aC_4H_7+CH_4$	8.0	8.20
$aC_3H_5 \rightarrow H+C_3H_4$	10.5	37.50	$iC_4H_8+CH_3 \rightarrow iC_4H_7+CH_4$	8.5	7.30
$C_3H_8 \rightarrow CH_3+C_2H_5$	16.3	84.50	$iC_4H_{10}+CH_3 \rightarrow iC_4H_9+CH_4$	10.0	9.00
$C_3H_6+H \rightarrow aC_3H_5+H_2$	9.4	1.10	$iC_4H_8+C_2H_3 \rightarrow iC_4H_7+C_2H_4$	9.0	13.00

Table A1. Continued

Reaction	Log A	E (Kcal/mol)
$iC_4H_{10}+C_2H_3\rightarrow iC_4H_9+C_2H_4$	9.0	16.80
$iC_4H_8+C_2H_5\rightarrow iC_4H_7+C_2H_6$	7.8	8.30
$iC_4H_{10}+C_2H_5\rightarrow iC_4H_9+C_2H_6$	9.2	10.40
$iC_4H_8+aC_3H_5\rightarrow iC_4H_7+C_3H_6$	8.3	13.50
$iC_4H_{10}+aC_3H_5\rightarrow iC_4H_9+C_3H_6$	9.0	19.00
$C_3H_6+1C_3H_7\rightarrow aC_3H_5+C_3H_8$	8.0	9.20
$C_3H_6+2C_3H_7\rightarrow aC_3H_5+C_3H_8$	8.0	10.20
$iC_4H_{10}+2C_3H_7\rightarrow iC_4H_9+C_3H_8$	9.3	31.50
$iC_4H_7\rightarrow 12C_3H_4+CH_3$	3.0	32.60
$iC_4H_7\rightarrow C_2H_4+C_2H_3$	12.0	28.00
$iC_4H_9\rightarrow iC_4H_8+H$	14.5	36.00
$iC_4H_9\rightarrow C_3H_6+CH_3$	13.9	33.00
$iC_4H_9\rightarrow 2C_4H_8+H$	13.6	36.60
$2C_4H_8+H\rightarrow 2C_4H_9$	9.8	1.20
$iC_4H_8+H\rightarrow iC_4H_9$	10.0	1.20
$12C_3H_4+CH_3\rightarrow iC_4H_7$	8.2	7.40
$C_3H_6+CH_3\rightarrow 2C_4H_9$	8.5	7.40
$iC_4H_8+CH_3\rightarrow C_5H_{11}$	8.0	7.20
$iC_4H_7+H\rightarrow iC_4H_8$	10.3	0.00
$iC_4H_9+H\rightarrow iC_4H_{10}$	10.0	0.00
$iC_4H_7+CH_3\rightarrow C_7H_{14}$	9.5	0.00
$iC_4H_7+aC_3H_5\rightarrow C_7H_{14}$	10.1	0.00
$nC_4H_{10}+H\rightarrow C_4H_9+H_2$	10.5	9.70
$nC_4H_{10}+H\rightarrow 2C_4H_9+H_2$	10.0	8.40
$nC_4H_{10}+CH_3\rightarrow C_4H_9+CH_4$	9.7	11.60
$nC_4H_{10}+CH_3\rightarrow 2C_4H_9+CH_4$	8.5	9.50
$nC_4H_{10}+C_2H_3\rightarrow C_4H_9+C_2H_4$	10.2	18.00
$nC_4H_{10}+C_2H_3\rightarrow 2C_4H_9+C_2H_4$	9.9	16.80
$nC_4H_{10}+C_2H_5\rightarrow C_4H_9+C_2H_6$	9.3	12.60
$nC_4H_{10}+C_2H_5\rightarrow 2C_4H_9+C_2H_6$	8.7	10.40
$nC_4H_{10}+aC_3H_5\rightarrow C_4H_9+C_3H_6$	8.6	18.80
$nC_4H_{10}+aC_3H_5\rightarrow 2C_4H_9+C_3H_6$	8.9	16.80
$nC_4H_{10}+1C_3H_7\rightarrow 2C_4H_9+C_3H_8$	8.3	10.40
$nC_4H_{10}+2C_3H_7\rightarrow 2C_4H_9+C_3H_8$	8.3	12.60
$C_4H_8\rightarrow C_4H_6+H_2$	4.0	18.10
$nC_4H_{10}\rightarrow C_2H_4+C_2H_6$	12.3	61.30

steady state assumption would be indeed valid as long as the coke formation rate does not change appreciably over a sufficiently small time step.

Material balance for component j:

$$\frac{dF_j}{dz}=(\sum_i s_{ij}r_{ri})\frac{\pi d_t^2}{4} \tag{1}$$

Energy balance in tube side:

$$\sum_j F_j c_{pj}\frac{dT}{dz}\equiv Q(z)\pi d_t+\frac{\pi d_t^2}{4}\sum_i r_{ri}(-\Delta H)_i \tag{2}$$

Momentum balance:

$$\left(\frac{1}{M_m P_t}-\frac{P_t}{\eta\cdot G^2 RT}\right)\frac{dp_t}{dz}=\frac{d}{dz}\left(\frac{1}{M_m}\right)+\frac{1}{M_m}\left(\frac{1}{T}\frac{dT}{dz}+Fr\right) \tag{3}$$

With the friction factor:

$$Fr=0.092\frac{Re^{-0.2}}{d_t}+\frac{\zeta}{\pi R_b} \tag{4}$$

And for the tube bends as:

$$\zeta=\left(0.7+.35\frac{\Lambda}{90^0}\right)\left(0.051+0.19\frac{d_t}{R_b}\right) \tag{5}$$

where R_b and Λ represents the radius of the tube bend and angle of bend, respectively. Since the coking is slow, quasi steady state conditions may be assumed, so that we can write the rate of coke formation:

$$\frac{\partial C}{\partial t}=(d_t-2t_c)\frac{\alpha r_c}{\rho_c} \tag{6}$$

Using the mathematical model, the amount of coke deposited on the internal wall of the reactor tubes has been calculated with a limiting value for tube skin temperature (1,100 °C). In the following, the effect of the coke thickness on the operating parameters has been demonstrated during the on-stream time of the furnace.

2. Kinetic Model Development

The reaction mechanism of thermal cracking is generally accepted as free-radical chain reactions. Many efforts have been made for the development of the reaction networks of the thermal cracking of gaseous feed. The radical reaction schemes for the cracking of normal and isoparaffins, and their mixture has been developed [Sundaram and Froment, 1978]. Also, a simulation program based on the fundamental free radical reaction kinetics was developed [Dente et al., 1979, 1983]. The aim of this study was to develop a complete mechanistic reaction network that could predict the behaviour of the cracking coils in different operating conditions with a feed of Ethane, Propane, n-Butane, i-Butane and their mixture. A simulation program of the reaction kinetics inside the coils of a thermal cracking unit can provide information on the effects of changing feed properties or alternative operating conditions on the thermal cracking product distribution. The experimental data obtained from free literature data [Vandamme et al., 1975; Sundaram and Froment, 1978; Towfighi et al., 1993], our pilot plant data and a large number of industrial results are used for the tuning of kinetic parameters.

A complete reaction network, using a rigorous kinetic model, for the decomposition of gaseous feed individually and their mixture such as LPG feed is developed, and is used for the simulation of a LPG cracker. The detailed mechanistic kinetic scheme in this simulation network, developed, involves 146 of reactions with molecular and radical species. As usual, this chain radical mechanism consists of several radical and molecular elementary reactions, which can be presented in Table A1.

The governing mass, energy, and momentum balance equations for the cracking coil constitute the boundary value problem which has a significant stiffness in numerical simulation due to the large differences in concentration gradient between radicals and molecules. This problem can be tackled through the application of the Gear method.

3. Coking Model

In olefin production using steam crackers, a carbonaceous material is deposited at the inner wall of the cracker coils and TLX tubes. This deposition, referred to as coking, is a very undesirable phenomenon, because it limits the on-stream time of the unit and reduces the overall ethylene selectivity. Coke formation in the pyrolysis of hydrocarbons is a complex phenomenon. Three mechanisms contribute to the deposition of a coke layer include catalytic coking,

asymptotic coking and condensation of polyaromatic [Towfighi et al., 2002]. Asymptotic coking is the main mechanism that occurs from the interaction between active sites on the coke layer with gas phase coke precursors. At the free radical sites unsaturated precursors from the gas phase react via addition, followed by a set of dehydrogenation and cyclization reactions finally yielding a graphitic coke layer. Several papers have been presented on cracking coil coking, and concluded that no existing model seems to be sufficient to describe all important aspects of coke formation during steam cracking with different feedstocks [Kopinke et al., 1993]. The present paper attends on the asymptotic coking mechanism and describes the development of a kinetic coking model in the pyrolysis of LPG. A number of coke precursors are found to contribute to the formation of coke. A literature survey and experimental data led to a coking model in which a number of coke precursors and the relative rates of coke deposition contribute to the formation of coke [Niaei et al., 2004]. The coke formation is first order with respect to the concentration of coke precursors. The precursors are classified into ethylene, propylene, butadiene, acetylene, aromatics (benzene, toluene, xylene, styrene). A reference component, ethylene is chosen in the group of coke precursors and the factors obtained from the relative coking rate [Tesner, 1984; Kopinke et al., 1988, 1993] as shown in Table 1.

Table 1. Relative rate constants of coke formation from unsaturated coke precursors

Coke precursors	Tesner [1984]	Kopinke [1993]
Ethylene	0.73	0.73
Propylene	0.41	0.83-1.09
Butadiene	1.56	1.68
Acetylene	11.7	7-20
Benzene	0.24	
Toluene	1.63	

The rate of coke formation expressed as first order reaction as below:

Ethylene → Coke
Propylene → Coke
Butadiene → Coke
Acetylene → Coke
Aromatics → Coke

Coking reaction constants are calculated at the gas/coke interface and thus for a higher temperature than in the bulk stream. The total rate of coke formation is expressed as:

$$r_c = \sum_{i=1}^{n} r_{c,i} \tag{7}$$

Since the coking is slow, quasi steady state conditions may be assumed, so that the deposition of coke can be shown as:

$$\frac{\partial C}{\partial t} = (d_t - 2t_c)\frac{\alpha r_c}{\rho_c} \tag{8}$$

Using the mathematical model, the amount of coke deposited on the internal wall of the reactor tubes has been calculated with a limiting value for tube skin temperature (e.g., for sample olefin plant is 1,100 °C). In the following, the effect of the coke thickness on the

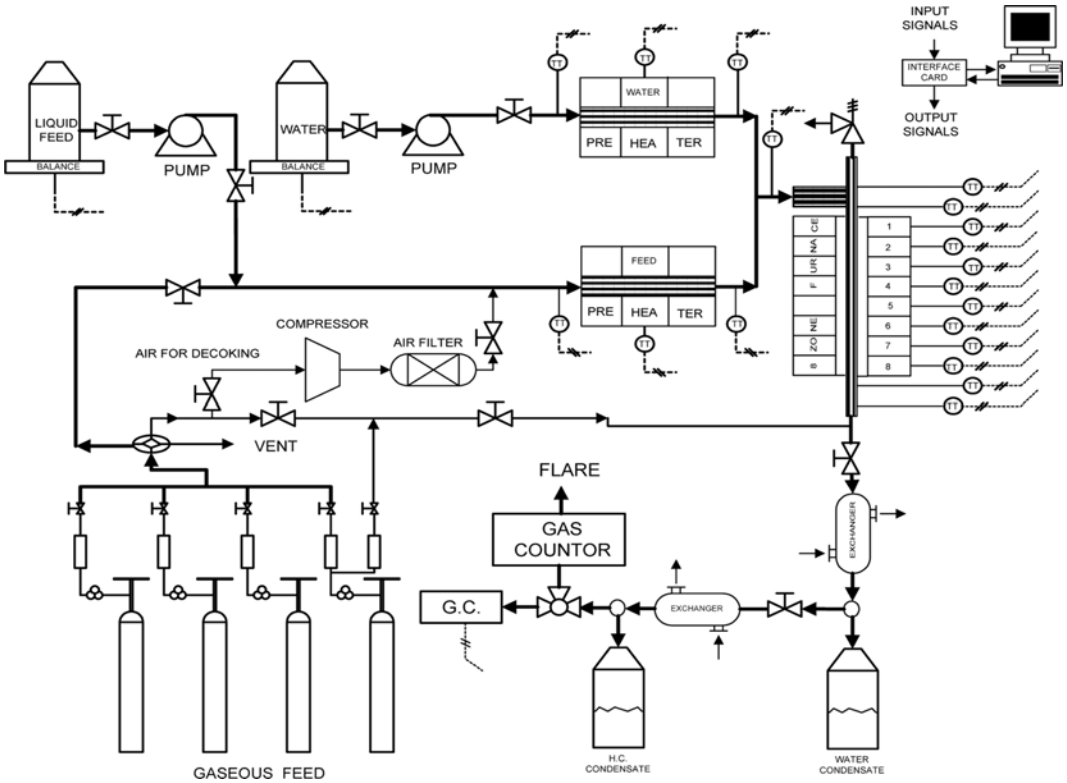

Fig. 1A. Schematic diagram of thermal cracking pilot plant.

operating parameters has been demonstrated in the on-stream time of the furnace.

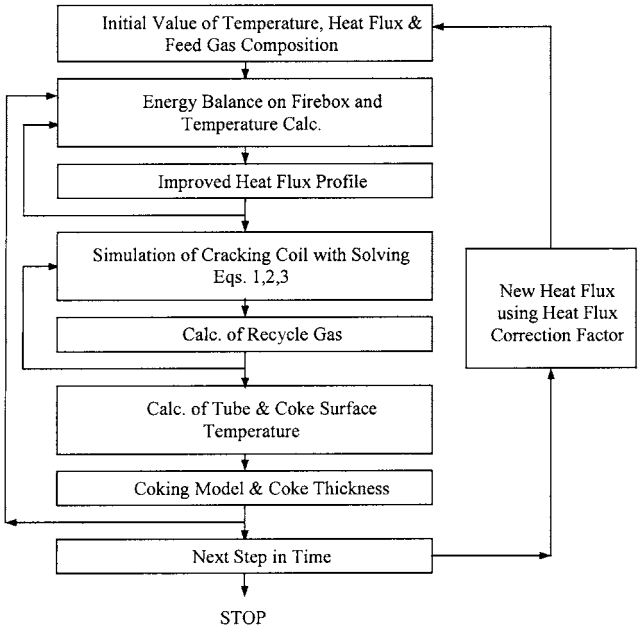

Fig. 2. Simplified flow chart of calculation of cracking coils.

4. Experimental Set Up

A pilot plant system was designed and assembled to study the pyrolysis reaction kinetics [Niaei et al., 2004]. The setup is a computer controlled pilot plant unit. Details of the pilot plant system are presented in ORG (Olefin Research Group) web site (http://www.modares.ac.ir/english/faculities/eng/olefin/index.htm). The hydro-

Table 2. Basic information of industrial cracking coil and firebox of gas cracker furnace

Reactor configuration		Feed composition (wt%)	
Total length (m)	89.4	Ethane	5.17
Internal diameter (mm)	108	Propane	16.85
External diameter (mm)	124	n-Butane	59.45
Number of burners	112	i-Butane	18.28
Operating condition			
Feed flow rate (Kg/day)	100,000	Coil outlet temp. (°C)	830
Coil inlet temp. (°C)	642	Dilution steam temp. (°C)	260
Steam to feed ratio (g/g)	0.3	Maximum skin temp. (°C)	1,100
Fuel composition (mol%)			
H_2	22.5	Excess air (%)	15
CH_4	65.5		
C_2H_6	12		

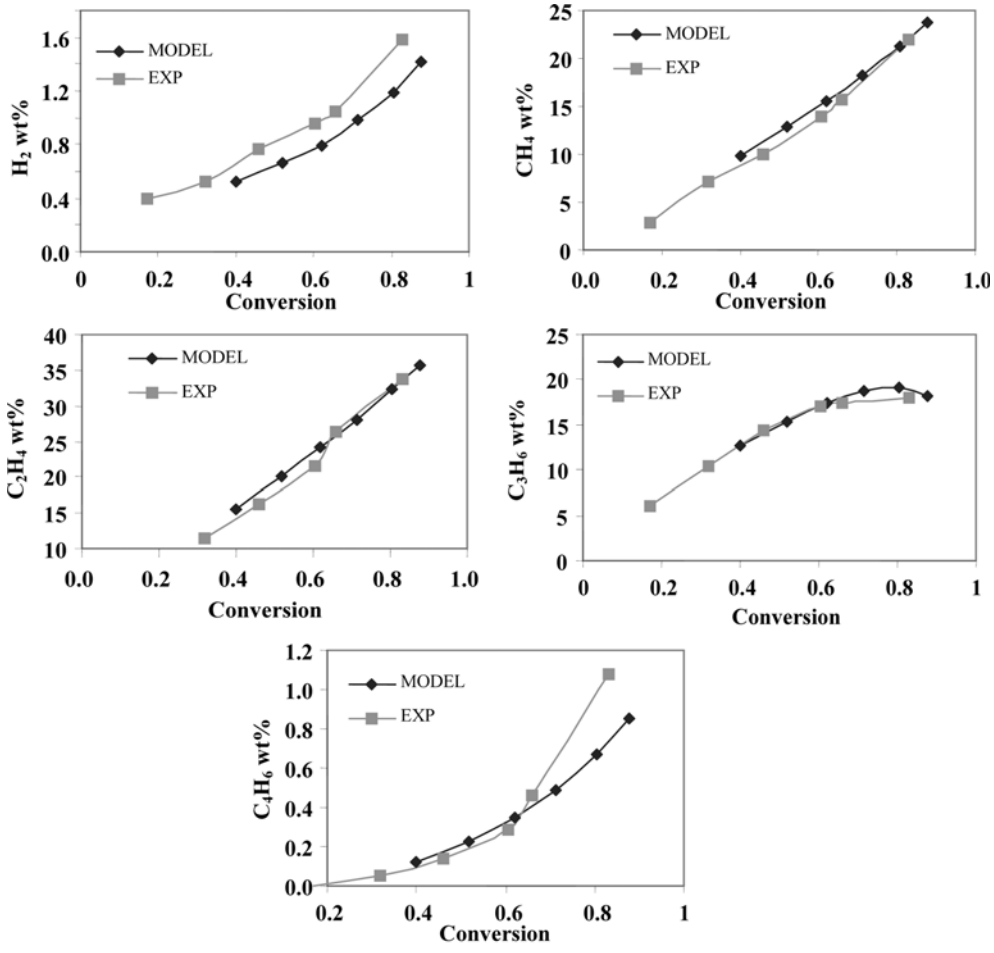

Fig. 3. Comparison of experimental & model product yields distribution in the thermal cracking of propane.

carbon and diluent water are heated to 600 °C in preheaters. The reaction section heater is divided into eight zones, which can be heated independently to set any type of temperature profile. Each zone power can be controlled by a control algorithm implemented on the process computer. The reactor is a 1 m long, 10 mm internal diameter tube, made of Inconel 600. There are eighteen thermocouples along the reactor, 8 inside the furnace, 8 on the external tube skin and additional 2 for measuring of XOT (Cross over temperature) and COT (Coil outlet temperature). The reactor is heated electrically and placed vertically in a cylindrical furnace. The analog signals of the thermocouples are connected to the process computer. The reactor effluent is cooled and separated by means of three glass condensers and cyclones. A fraction of the product gas is then withdrawn for the analysis, while the rest is sent to the flare. The on-line analysis of the reactor effluent is performed by means of two computerized Varian Chrompack CP3800 gas chromatographs, which analyse the cracked gases and condensate (Fig. 1A).

A process computer connected on-line to the pilot plant controls the main part of the unit. The connection with the pilot plant is done through analog to digital (A/D) converters, digital to analog (D/A) converters, and digital input-outputs. The temperature profile of the reactor is stabilized by temperature control in each zone by means of a conventional PID controller. The set points for this temperature stabilizing control are included in the software. All pilot plant measurements and control system information are saved in text and graphical mode.

5. Simulation Procedure

A simplified flowchart of the iterative calculation scheme is given in Fig. 2. Predicting the run length of the industrial cracking furnace requires the simultaneous solution of the rigorous kinetic model for the pyrolysis of hydrocarbons, coking model and energy balance in the fire box. To do so, the run time is increased in a stepwise manner. Incremental pseudo steady state is assumed for the coking, since the main cracking reactions are much faster than the coke formation. Starting from initial estimates for temperatures, fluxes and recycle gas composition, the energy balances, are solved and better estimates for the firebox temperature provided. From the tube skin and process gas temperatures, new flux estimates are calculated. Table 2 represents the basic information about the sample industrial gas cracking coils, the split coil reactors and the operating conditions.

The model and experimental product distribution for the main products of pyrolysis of propane, n-butane and i-butane are compared in Figs. 3-5.

Fig. 6 shows the evolution of the external wall, internal wall, coke surface and process gas temperature profiles along the cracking coils. In the first part of the reactor, the temperature profile shows a sig-

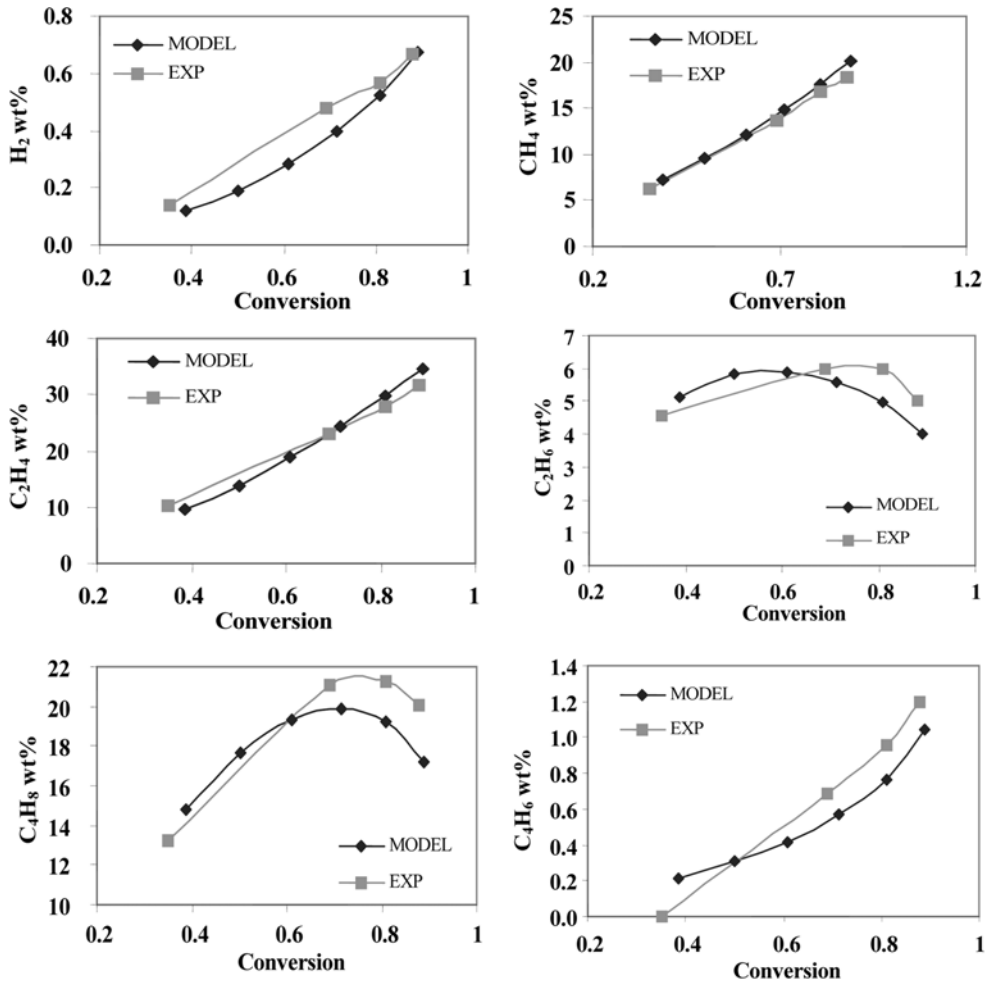

Fig. 4. Comparison of experimental & model product yields distribution in the thermal cracking of n-butane.

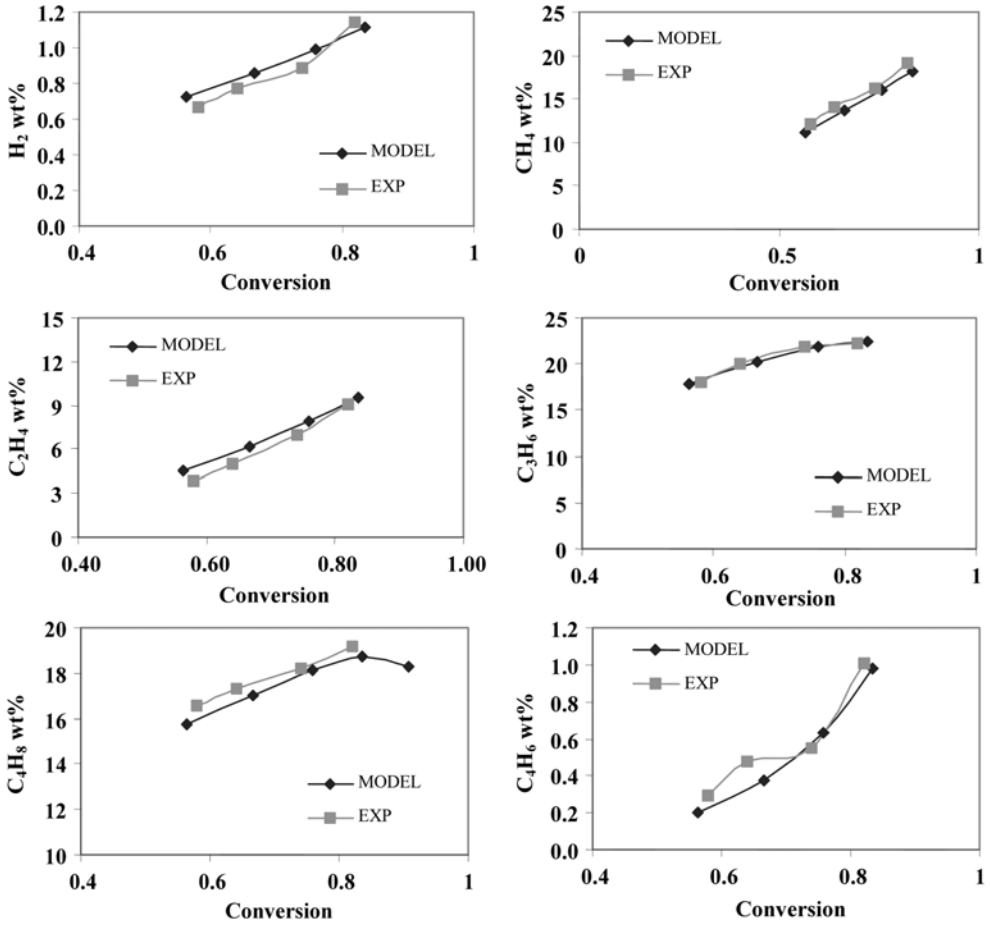

Fig. 5. Comparison of experimental & model product yields distribution in the thermal cracking of i-butane.

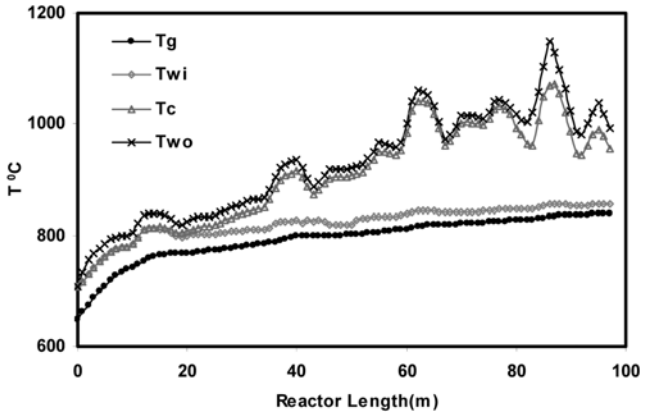

Fig. 6. Axial process gas (T_g), coke surface (T_c), inner tube wall (T_{wi}) and external tube skin (T_{wo}) temperature profile.

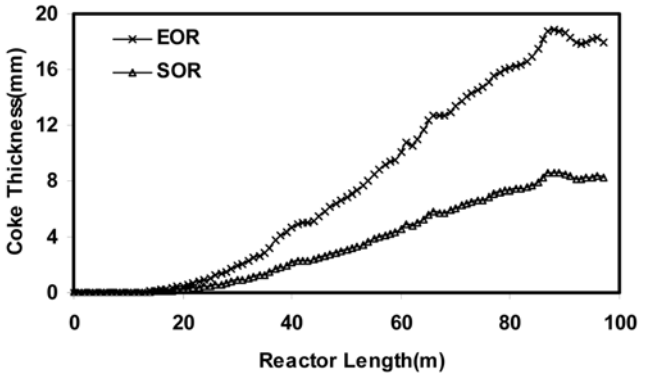

Fig. 7. Variation of coke thickness profile in the length of reactor at the end of run time.

nificant increase as well, but this is mainly due to the higher heat flux. The peaks in the external and internal tube skin temperature profile correspond with the bottom of the furnace.

The maximum value is reached at the end of coil. The axial tube skin temperature profile follows the shape of the heat flux profiles. The temperature peaks are important for the choice of the tube material. The coke surface temperature profile follows the shape of the tube skin temperature profile and the profile of coke thickness along the coil. The formation and deposition of coke on the inner surface of the coil has major consequences on the operation of the furnace. The coke layer reduces the heat transfer from the furnace to the process gas. The process gas temperature is relatively insensitive to the heat flux variations. This is due to the high mass flow rate in the reactor, which dampens changes in heat input, and to the endothermic nature of the pyrolysis process, that has a self stabilizing effect on the process gas temperature.

Fig. 7 shows the simulated coke layer thickness as a function of the length of reactor. The coke formation takes place at the temper-

ature of the gas/coke interface. As a consequence, the coke layer grows fast there and creates an additional resistance to the heat transfer and causes a decrease of the tube cross sectional area. Increasing the heat fluxes increases the gas/coke interface temperatures and the coking rates. The coke deposition reaches its maximum thickness in the last pass at the end of reactor. The on-stream time of cracking furnace is limited by the external tube skin temperature. In the present investigation the maximum allowable temperature at the second part of coil is 1,100 °C. The simulated value is in agreement with the industrial plant data. The tube skin temperatures are measured by a pyrometer.

INDUSTRIAL CASE SYUDY

In Figs. 8-10 the yields of main cracking products are plotted against the severity index. We obtained these results for the cracking of LPG (with different %wt of mixture of propane, i-butane and n-butane in the feed; main part) at different severity index or coil outlet temperatures. In general, with increase of severity, the yield of propylene increases and thermally stable methane, ethylene and aromatic yields will be slightly decreased. In our experimental process, the above-mentioned trend has been also observed. The calculated values from the kinetic reaction network which has been developed in ORG for each product yield in LPG pyrolysis are in good agreement with the plant data.

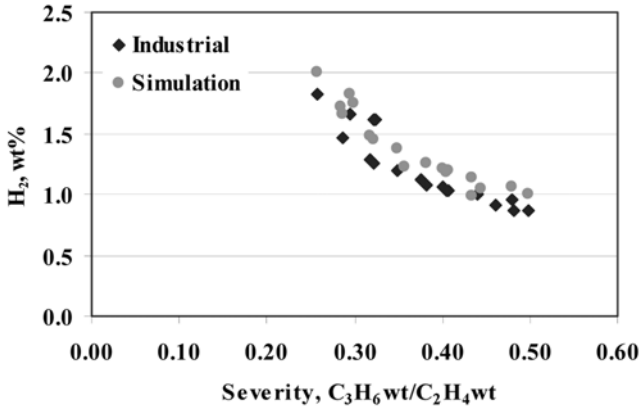

Fig. 8. Hydrogen yield vs. severity (plant data/simulation results).

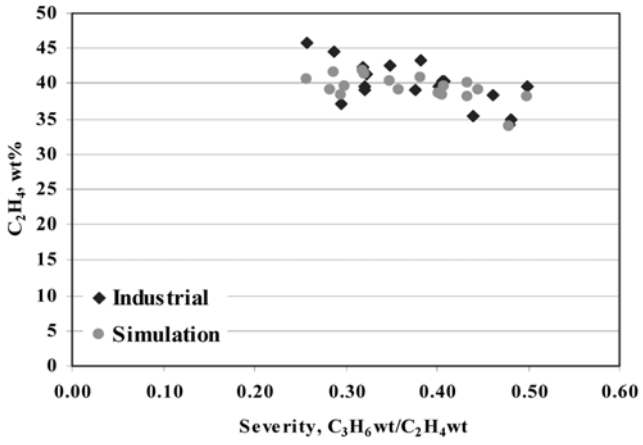

Fig. 9. Ethylene yield vs. severity (plant data/simulation results).

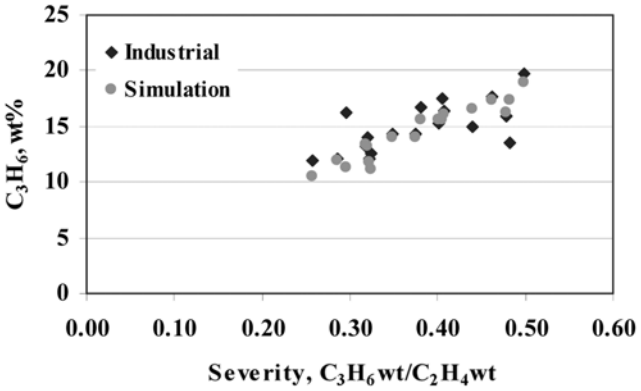

Fig. 10. Propylene yield vs. severity (plant data/simulation results).

The present work is concerned with the modelling and simulation of an LPG cracking furnace. With the help of a kinetic reaction network for the pyrolysis of ethane, and an accurate coking kinetic model, an industrial cracking furnace is simulated. Pyrolysis reaction kinetic parameters of LPG were tuned and verified with large amounts of industrial data. Simultaneous simulation of the reactor and the firebox provides a detailed understanding of the behaviour of the cracking furnace such as gas temperature and product distribution in the reactor length and run time can be achieved.

CONCLUSION

A complete reaction network, using a rigorous kinetic model, for the decomposition of gaseous feed of Ethane, Propane, n-Butane, i-Butane and their mixture individually is developed, and is used for the simulation of an LPG cracker. A simulation program of the reaction kinetics inside the coils of a thermal cracking unit can provide information on the effects of the feed properties or alternative operating conditions on the thermal cracking product distribution. With the help of an accurate simulation of a pyrolysis reactor in a cracking furnace, the distribution of the product yields, temperature and heat flux distribution in the reactor can be achieved. The simulated and plant observation run lengths are in good agreement. Simulations of this kind can be used to design and optimise furnace operation for various feedstock, firing conditions and operating conditions. The growth of a coke layer is accurately simulated, and so is the evolution of the external tube skin temperatures. This simulation can be used as a guide for the adaptation of the operating variables aimed at prolonging the run length of the furnace. The model and simulation software presented here are used as a guide for plant operation in an olefin plant to control the furnace parameters.

ACKNOWLEDGMENT

The authors acknowledge the support given by olefin units of BIPC & Abadan petrochemical companies of Iran.

NOMENCLATURE

C : accumulation of coke [m]
C_i : concentration of coke precursors [mole/m^3]

Cp : heat capacity [J/mole·K]
d_t : tube diameter [m]
E : activation energy [J/mole]
F : molar flow rate [mole/hr]
G : total mass flux of the process gas [kg/m^{2}s]
$-\Delta H$: heat of reaction [J/mole]
k : thermal conductivity of tube [W/m·K]
M_m : average molecular weight [kg/mole]
N : reaction order for coking
P_t : total pressure [Kpa]
Q : heat flux [W/m^2]
R_b : radius of the tube bend [m]
R : tube radius [m]
r_c : coking reaction rate [kg/m^{3}s]
r_{ri} : reaction rate in pyrolysis process [mole/m^{3}s]
t_c : coke thickness [m]
t : time [hr]
s_{ij} : stoichiometry factor
T : temperature [K]
Z : axial reactor coordinate [m]

Greek Letters

α : coking factor
Λ : angle of bend 0
ρ_c : coke density [kg/m^3]
η : unit conversion factor

Abbreviations

n : normal
a : alyl
i : iso
SOR : start of run
EOR : end of run

REFERENCES

Dente, M. and Ranzi, E., *Pyrolysis. Theory and industrial practice*, Albright, L. F., Crynes, B. L. and Corcoran, W. H., Chapter 7, Academic Press, New York, USA (1983).

Dente, M., Ranzi, E. and Goossens, A. G., "Detail prediction of olefin yields from hydrocarbon pyrolysis through a fundamental simulation model (SPYRO)," *Comput. Chem. Eng.*, **3**, 61 (1979).

Froment, G., Van de Steene, B. O. and Van Damme, P., "Thermal cracking of ethane and ethane-propane mixtures," *Ind. Eng. Chem. Process Des. Dev.*, **15**, 495 (1976).

Heyndericks, G. J. and Froment, G. F., "Simulation and comparison of the run length of an ethane cracking furnace with reactor tubes of circular and elliptical cross sections," *Ind. Eng. Chem. Res.*, **37**, 914 (1998).

Kopinke, F. D., Zimmermann, G., Reyners, G. C. and Froment, G. F., "Relative rates of coke formation from hydrocarbons in steam cracking of naphtha. 2. Paraffins, naphthenes, mono, Di and cycloolefins and acethylenes," *Ind. Eng. Chem. Res.*, **32**, 56 (1993).

Kopinke, F. D., Zimmermann, G. and Nowak, S., "On the mechanism of coke formation in steam cracking conclusions from results obtained by tracer experiments," *Carbon*, **56**(2), 117 (1988).

Niaei, A., Towfighi, J., Sadrameli, M. and Karimzadeh, R., "The combined simulation of heat transfer and pyrolysis reactions in industrial cracking furnaces," *Applied Thermal Engineering*, **24**, 2251 (2004).

Sundaram, K. M. and Froment, G., "Modeling of thermal cracking kinetics. 3. Radical mechanisms for the pyrolysis of simple paraffins, olefins, and their mixtures," *Ind. Eng. Chem. Fund.*, **17**(3), 174 (1978).

Tesner, P. A., "Kinetics of pyrolysis carbon formation," *Chemistry and Physics Carbon*, **19**, 65 (1984).

Towfighi, J., Sadrameli, M. and Niaei, A., "Coke formation mechanisms and coke inhibiting methods in pyrolysis furnaces," *Journal of Chem. Eng. of Japan*, **35**(10), 923 (2002).

Towfighi, J., Nazari, H. and Karimzadeh, R., *Simulation of light hydrocarbons pyrolysis using radical mechanism*, APCChE/CHEMECA 93, Melbourne, Australia (1993).

Van Damme, P. S. and Froment, G. F., "Scaling up of naphtha cracking coils," *Ind. Eng. Chem. Proc. Des. Dev.*, **20**, 366 (1981).